TURBULENCE STUDIES IN TOKAMAK BOUNDARY PLASMAS WITH REALISTIC DIVERTOR GEOMETRY*

X.Q. XU, R.H. COHEN, G.D. PORTER, T.D. ROGNLIEN, D.D. RYUTOV,
J. R. MYRA[1], D. A. D'IPPOLITO[1], R. MOYER[2], R. J. GROEBNER[3]

Lawrence Livermore National Laboratory,
Livermore, California,
United States of America

Abstract

Results are presented from the 3D nonlocal electromagnetic turbulence code BOUT [1] and the linearized shooting code BAL[2] for studies of turbulence in tokamak boundary plasmas and its relationship to the L-H transition, in a realistic divertor plasma geometry. The key results include: (1) the identification of the dominant resistive X-point mode in divertor geometry and (2) turbulence suppression in the L-H transition by shear in the $\mathbf{E}\times\mathbf{B}$ drift speed, ion diamagnetism and finite polarization. Based on the simulation results, a parameterization of the transport is given that includes the dependence on the relevant physical parameters.

1. Boundary Plasma Turbulence Studies

BOUT models the boundary plasma that spans the separatrix using fluid equations for plasma vorticity, density, ion temperature and parallel momentum, and electron temperature and parallel momentum. The equations are those of Ref. [3], extended to include the magnetic pumping by replacing the scalar pressure with the anisotropic pressure $\overleftrightarrow{\mathbf{P}}_i = P_i\overleftrightarrow{\mathbf{I}} - 3\eta_0((V_{E\times B}+V_{\nabla P_i})\cdot\nabla\ln B)(\mathbf{bb}-\overleftrightarrow{\mathbf{I}})$, where η_0 is the classical parallel viscosity. This reduced equation set includes the well-known linear instability drives for (1) conducting-wall modes, (2) Kelvin-Helmholtz modes, (3) curvature-driven ideal-MHD-ballooning and resistive ballooning modes, (4) resistive drift-Alfven modes, (5) $\nabla_x v_{||}$ modes, and (6) axial shear modes ($\nabla_{||}\mathbf{v_{E\times B}}$). In order to investigate pedestal physics, we first run the edge plasma transport code UEDGE/EFIT to get the X-point magnetic geometry and plasma profiles.

The BAL code is a linear eigenvalue code that solves a similar set of fluid equations on field lines in the edge and SOL plasma for realistic X-point geometry. The code is eikonal, and retains drift, resistive and collisionless skin effects. We employ BAL to gain insight into the physics of the underlying linear instabilities in boundary plasmas, to benchmark the 3D turbulence code BOUT, and to search for various instability thresholds.

In an X-point divertor geometry, the local pitch $q(r,\theta)$ varies along the magnetic field line and there exists a steep parallel gradient of q near the X-point. There are two effects: (1) the local magnetic shear $\hat{s}(r,\theta)$ becomes large near the X-point; (2) the magnetic connection length ($L_{||}\sim q(r,\theta)R$) becomes long when a flux tube passes near an X-point. The first effect can yield rapid mode oscillation along the field line near the X-point, in which case the validity of the eikonal representation becomes questionable. However, the parallel electron viscous damping and heat conduction terms smooth rapid $k_{||}$ variations near the X-points. In the electromagnetic regime ($\epsilon = k_\perp^2 c^2/\omega_{pe}^2 < 1$), we find that normally the dissipation terms are smaller than the others by $\mathcal{O}(\epsilon)$. However, near the X-point(s), ϵ may exceed one because k_r is large, dissipation can become important, and the modes become electrostatic. The localization of dissipation and electron skin effects near the X-points enables resistive curvature driven modes with strong drive near the X-point(s). This physics profoundly affects the unstable spectrum, and generally results in modes localized between the upper and lower X-points on the low-field-side. We refer to such mode as

* Work performed for USDOE under contracts W-7405-ENG-48 at LLNL, DE-FG03-97ER54392 at LRC, DE-FG03-95ER54294 at UCSD. [1]Lodestar Research Corporation, Boulder, CO 80301 USA; [2]University of California, San Diego, La Jolla, CA 92093 USA; [3]General Atomics, San Diego, CA 92186 USA

"*resistive X-point modes*". The eigenmode structure from a typical BOUT simulation is shown in Fig. 1.

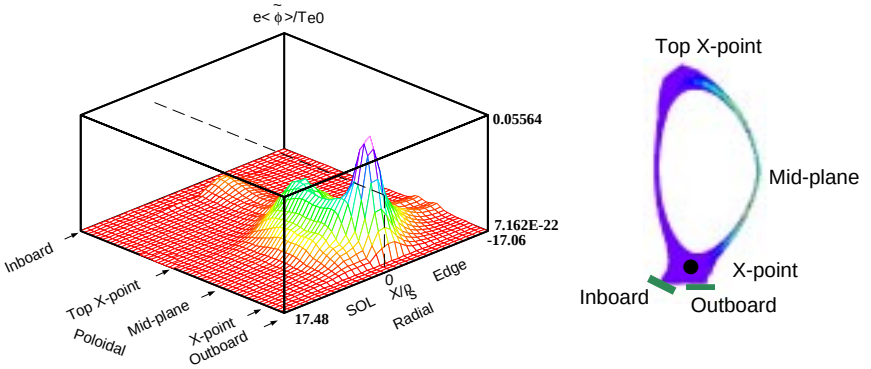

Fig.1. Fluctuating potential $e\langle\tilde{\phi}\rangle_\varphi/T_{e0}$ *in 2D radial and poloidal plane from a typical BOUT simulation.*

The fluctuating potential is peaked near the low X-point just inside the separatrix. As shown in Fig. 1, even though the configuration is a single null divertor, there is still an X-point near the scrape-off-layer (SOL) on the top of the machine, and its magnetic shear limits penetration of the fluctuations into the inside of the torus. BOUT runs with the curvature term turned off show a significant reduction of the linear-instability growth rate. Linear eikonal ballooning analysis (BAL) also shows that the X-point dramatically affects the eigenfunction shape and unstable spectrum. Fig. 2 shows the eigenfunction and linear growth rate in the SOL with and without X-points (in the latter case, B_p and magnetic shear $\hat{s}$ are set to their mid-plane values).

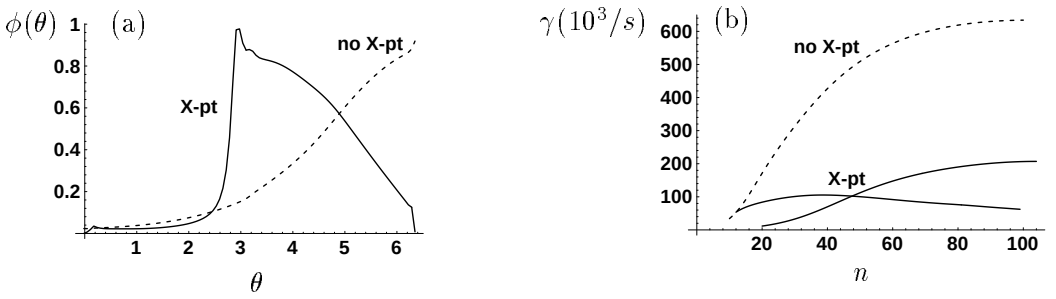

Fig.2. (a). Fluctuating potential $\tilde{\phi}(\theta)$ *vs. poloidal angle* θ *with (solid line) and without (dashed line) X-point.* θ *increases from inboard to outboard as Fig.1. The top X-point is at* π*; (b). Linear growth rate* γ *vs. toroidal mode number n with X-points (solid lines) and without them (dashed line).*

The fluctuation peaks near the X-points and the linear growth rate is typically smaller with the X-point present. In the case without X-points, the eigenfunction peaks near where the lower X-point would have been since the curvature drive is strong there; the conducting-wall-mode drive is destabilizing, but is subdominant. The frequency spectra of the mid-plane particle flux from probe measurements and BOUT simulations in L mode shows reasonable agreement [3].

2. L-H Transition

For given DIII-D discharge 89840, we analyze the instabilities and turbulence at two different time slices 2370ms and 2470ms, corresponding to L and H mode. We obtain equilibrium plasma profiles by using hyperbolic tangent fits to the mid-plane experimental data for the plasma density N_{i0}, electron temperature T_{e0}, ion temperature T_{i0} and assuming uniform profiles along the field line. We find that there is little change in the magnetic geometry between L and H mode. The plasma density N_{i0} is radially steeper by a factor of 4, the ion temperature is steeper by a factor of 2, and the electron temperature is steeper by a factor of 1.5 in H mode.

From BAL calculations, we find that in the DIII-D H phase, the ideal MHD edge ballooning mode is near the marginal stability boundary and is a good candidate for the quasi-coherent mode

seen in the experiments [4]. In both the L and H phases, a broad range of unstable toroidal mode numbers n was found for resistive X-point modes, in the range $n \sim 30 - 400$. The most linearly unstable growth rate and mode number n have been benchmarked between BOUT and BAL in the L-mode phase. After averaging the linear growth rate on different flux surfaces from BAL over a half radial mode width from BOUT, the two codes agree very well.

In order to investigate the physics influences on the electric field E_r, we start from the Braginskii force balance equation:

$$\mathbf{E}_\perp = \frac{\mathbf{1}}{\mathbf{Z}_\alpha \mathbf{e} \mathbf{n}_\alpha} \nabla \cdot \overleftrightarrow{\mathbf{P}}_\alpha - \frac{\mathbf{1}}{\mathbf{c}} \mathbf{V}_\alpha \times \mathbf{B} - \frac{\mathbf{m}_\alpha}{\mathbf{Z}_\alpha \mathbf{e}} \left(\frac{\partial \mathbf{V}_\alpha}{\partial \mathbf{t}} + \mathbf{V}_\alpha \cdot \nabla \mathbf{V}_\alpha \right) \tag{1}$$

This equation can be separated into equilibrium and turbulent parts $\mathbf{E}_\perp = \mathbf{E}_{\perp \mathbf{0}} + \delta \mathbf{E}_\perp$:

$$\mathbf{E}_{\perp \mathbf{0}} = \frac{\mathbf{1}}{\mathbf{Z}_\alpha \mathbf{e} \mathbf{n}_\alpha} \nabla \cdot \overleftrightarrow{\mathbf{P}}_{\alpha \mathbf{0}} - \frac{\mathbf{1}}{\mathbf{c}} \mathbf{V}^{\mathbf{0}}_\alpha \times \mathbf{B}_\mathbf{0} \tag{2}$$

$$\delta \mathbf{E}_\perp = \frac{\mathbf{1}}{\mathbf{Z}_\alpha \mathbf{e} \mathbf{n}_\alpha} \nabla \cdot \delta \overleftrightarrow{\mathbf{P}}_\alpha - \frac{\mathbf{1}}{\mathbf{c}} \delta \left(\mathbf{V}_\alpha \times \mathbf{B} \right) - \frac{\mathbf{m}_\alpha}{\mathbf{Z}_\alpha \mathbf{e}} \left(\frac{\partial \delta \mathbf{V}_\alpha}{\partial \mathbf{t}} + \delta (\mathbf{V}_\alpha \cdot \nabla \mathbf{V}_\alpha) \right) \tag{3}$$

The equilibrium electric field $\mathbf{E}_{\perp \mathbf{0}}$ is calculated either from measured plasma profiles or from the edge plasma transport code UEDGE [5] (which solves the current continuity equation $\nabla \cdot n_i e(\mathbf{V}_i^0 - \mathbf{V}_e^0) = 0$ with $\mathbf{V}_\perp^0$ iteratively determined from Eq. (2)). Instead of calculating $\delta \mathbf{E}_\perp$ from Eq. (3), the turbulent $\delta\phi$ is obtained from quasineutrality ($\delta n_e = \delta n_i$); substituting Eq. (3) for the electron and ion species into the current continuity equation ($\nabla \cdot \delta \mathbf{J} = \mathbf{0}$) gives the vorticity equation. The calculated electric field E_r on the mid-plane from BOUT is given in Fig. 3 for the H-mode phase.

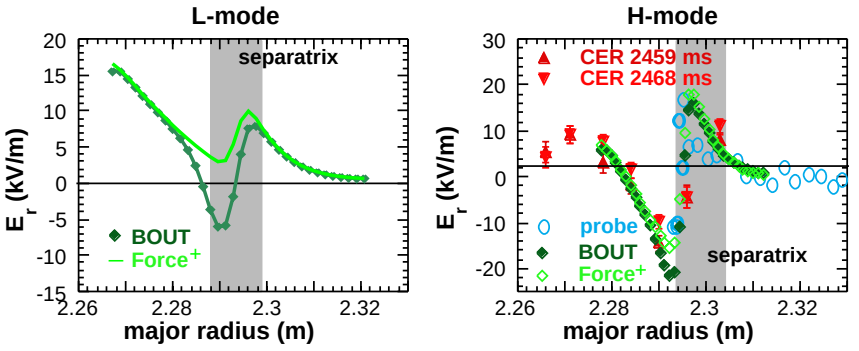

Fig.3. Electric field $E_r(x)$ from BOUT simulations. The filled diamonds are the computed $E_r(x)$ including the turbulence-generated contribution; the Force$^+$ is the equilibrium electric field calculated from Eq. (2) inside the separatrix and the sheath potential in the SOL; The triangles are the result from CER measurements; the open circles are the result from Langmuir probe measurements.

It is shown that the overall radial profile of E_r is determined by the *equilibrium* force balance equation; however, the turbulence produces significant contribution just inside the separatrix. The E_r in L-mode is small and positive. The turbulent suppression of the fluctuating potential $\langle\tilde{\phi}\rangle_{rms}$ and the ion heat diffusivity χ_i are shown in Fig. 4.

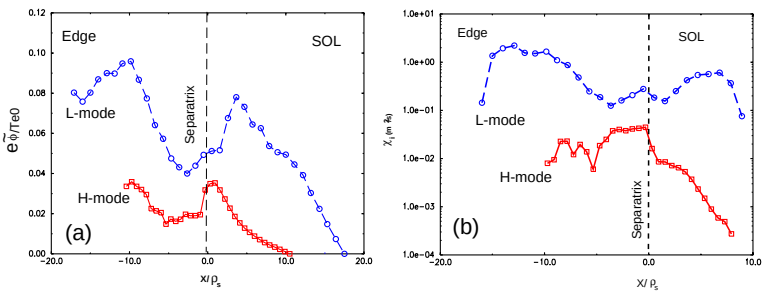

Fig.4. (a) Electrostatic potential fluctuations $e\langle\tilde{\phi}\rangle_\varphi / T_{e0}$ across the separatrix measured at mid-plane from BOUT simulations; (b) Turbulence-generated ion heat diffusivity χ_i from BOUT simulations.

Even in the absence of flow shear, the SOL transport is moderated due to finite ion diamagnetism and finite-polarization-stabilization of SOL modes [6]. Flow shear reduces turbulence both in the SOL and edge regions[7][8].

3. L-mode Transport Scalings

The turbulent transport fluxes can be expressed in the form: , $= \psi_0 c_s F(\hat{\beta}, \rho_s/R_0, L_\perp/\rho_s, L_{||}/\rho_s, \hat{s}, \hat{\nu}, \Lambda)$. Here ψ_0 is the density N_0, electron temperature T_{e0}, ion temperature T_{i0} or parallel velocity $V_{||i0}$ for the corresponding flux, and $L_\perp$ represents the set of scale lengths of density, temperature, parallel velocity and ion pressure gradient perpendicular to $\mathbf{B}$. F is a dimensionless function of the dimensionless arguments determined from theoretical arguments and/or from simulations. The dependence of , on $\hat{\beta}$ and ν_{ei} is plotted in Figs. 5. The base case $\hat{\beta}_0$ and ν_{ei0} correspond to DIII-D L-mode phase. In $\hat{\beta}$ scans of the transport, the linear instability drivers and the magnetic equilibria are fixed. The dependence of , on other parameters will be reported in future publications.

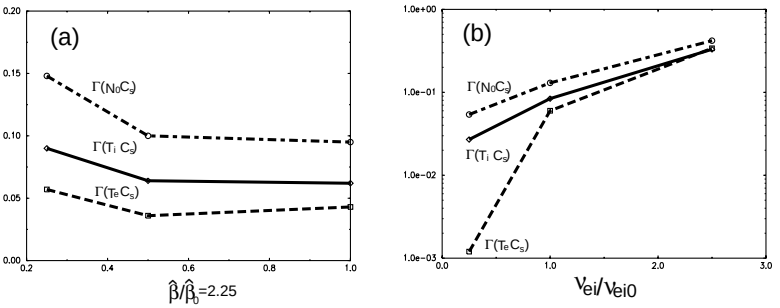

Fig.5. Scaling of the $\mathbf{E} \times \mathbf{B}$ *contribution to turbulent transport fluxes* , *with (a)* $\hat{\beta} = \beta/2\mu_e, \mu_e = m_e/M_i, \beta = 8\pi n T_e/B^2$*; (b) electron-ion collisionality* ν_{ei}*.*

4. Summary

Our 3D nonlocal fluid turbulence simulations of boundary plasmas have been extended into the experimentally relevant X-point divertor geometry. A broad range of high toroidal mode number n for resistive X-point turbulence is found in the range $n \sim 30 - 400$ both for L-mode and H-mode. The localization of electron skin effects near the X-points enables resistive curvature driven modes with strong drive near the X-point(s). Flow shear is found to be the dominant mechanism for the suppression of boundary turbulence, though finite polarization and ion diamagnetism also contribute, especially in the SOL. Turbulence produces a visible radial electric field E_r just inside the magnetic separatrix. The scaling scans of the transport show the sensitivities of , on $\hat{\beta}$ and ν_{ei}.

REFERENCES

[1] Xu, X. Q., and Cohen, R. H., Contributions to Plasma Physics, June(1998).
[2] Myra, J. R., D'Ippolito, D. A., and Goedbloed, J. P., Physics of Plasmas, Vol.**4** 1330-1341(1997).
[3] Xu, X. Q., Cohen, R. H., Porter,G. D., Myra, J. R., D'Ippolito, D. A., Moyer, R., 13th Iternational Conference on Plasma Surface Interactions in Controlled Fusion Devives, San Diego, California, May(1998).
[4] Moyer, R., et al., 13th Iternational Conference on Plasma Surface Interactions in Controlled Fusion Devives, San Diego, California, May(1998).
[5] T.D. Rognlien, G.D. Porter, and D.D. Ryutov, 13th Iternational Conference on Plasma Surface Interactions in Controlled Fusion Devives, San Diego, California, May(1998).
[6] Cohen, R. H., and Xu, X. Q., Physics of Plasmas Vol.**2** 3374-3383(1995).
[7] Biglari, H., Diamond, P. H., and Terry, P. W., Phys. Fluids **B 2** (1990) 1.
[8] Burrell, K. H.,Physics of Plasmas Vol.**4** (1997) 1499.